

Proceedings of 7th Transport Research Arena TRA 2018, April 16-19, 2018, Vienna, Austria

Reduced-scale power hardware-in-the-loop simulation of a hybrid railway power substation

Nanfang Yang a, Tony Letrouvé a*, Cristian Jecu b, Löic Joseph-Auguste b,
Julien Pouget a

^aSNCF Innovation & Recherche, 40 avenue des Terroirs de France, 75611 Paris, France

^bEDF R&D, avenue des Renardières, 77250 Moret-sur-Loing, France

Abstract

With the growth of the passenger flow in railway transportation system in France, some railway substations are approaching their power limits, thus have difficulty to reinforce the power supply. The substation upgrade usually requires changing power transformers and connecting cables, thus costly. The integration of renewable energies and storage system to form a hybrid railway power substation (HRPS) could be a good solution, which can satisfy the power requirement with smaller investment, and also opens an opportunity to participate into the electricity market. Instead of build the prototype directly, this paper proposes a reduced-scale power hardware-in-the-loop (HIL) simulation platform to verify the technical availability of HRPS.

Keywords: Hardware-in-the-loop; railway power substation; renewable energy; energetic macroscopic representation (EMR).

* Corresponding author. Tel.: +33-157-236-251.
E-mail address: tony.letrouve@sncf.fr

1. Introduction

Railway transportation system is an economic, efficient and environment-friendly passenger transport way. In France more than 100 billion passenger-km is transported by railway system in 2014, including train, tramway, and metro, which takes over 10% of the total passenger-km and increases progressively (Commissariat général au développement durable, 2016). With the growth of railway traffic flow, the Railway Power Substation (RPS) is approaching its power limit, this implies a lower limit for the running speed of trains, thus reduces the line capacity. Besides, the energy efficiency improvement and reduction of CO₂ are also very important topics for train manufacturers as well as railway operators. For example, SNCF has set the objective to reduce 20% of energy consumption (electricity and diesel) between 2012 and 2020 and 25% of CO₂ emissions between 2014 and 2025 (SNCF).

To enhance the power supplied by catenary and RPS, autotransformer based 2×25 kV AC line or even new RPS are required to be constructed, however costly. The integration of renewable energy sources as well as energy storage system to achieve a microgrid could be a good solution for this problem. Many studies and demonstrated projects have been conducted to integrate on-board or wayside energy storage system, mainly aiming to recover regenerative braking energy and improving energy efficiency. This is very useful for the DC line, because the rectifier used in DC type RPS doesn't allow energy to be fed back to electric grid. Besides, the on-board energy storage can also support catenary-free operation or emergency operation when the catenary/feeder is unavailable. While the wayside energy storage can enable not only regenerative braking energy recuperation but also upstream electric grid service such as peak load shaving or other load-side demand-response (Radcliffe, Wallace, & Shu, 2010). It has been reported that a way-side Nickel-Metal hydride (Ni-MH) battery can recycle as high as 71.4% of the regenerative braking energy in DC railway system (Ogura, et al., 2011).

The integration of energy storage and renewable energy sources in the traditional RPS can form a Hybrid RPS (HRPS) (Pankovits, et al., 2013) or railway microgrid (Nasr, Iordache, & Petit, 2015). This multiple energy sources system requires an efficient EMS to enable the optimal operation of HRPS, especially in the context of liberate electricity market. However the test and verification of HRPS management system requires a prototype to be constructed in advance, if the traditional development path is applied. This is time-consuming, costly and also unrealistic for the project. Hardware-in-the-Loop (HIL) can be adopted to reduce the development time and cost, to enable the verification of EMS before deployment on site. This paper focuses on modelling and HIL test of an AC type HRPS, to supply a test bench for Energy Management System (EMS) development. At first the structure of HRPS will be introduced, and then the mathematical model of each element will be built to obtain a HRPS model. Then, reduced-scale Power HIL with a lead-acid battery will be constructed in our laboratory to confirm its effectiveness.

2. AC type hybrid railway power substation

The railway power system can be divided into two types: DC line system and single-phase AC line system. The AC line has the voltage of 25kV/50Hz and usually for high-speed trains in France, such the national line LN1 between Paris and Lyon. A simple single-phase railway power supply architecture is given in Fig. 1. The AC type RPS usually takes power directly from two separate transmission grids (only one is demonstrated in Fig. 1) and then power the single-phase catenary through two power transformers. The two transforms work in turn and backup for each other. An AC RPS can supply power for a section around 40 to 60 km, and a neutral section is mandatory between two sections because the nearby RPSs are tied to different phases of the transmission line to limit unbalancing in the upstream electric grid.

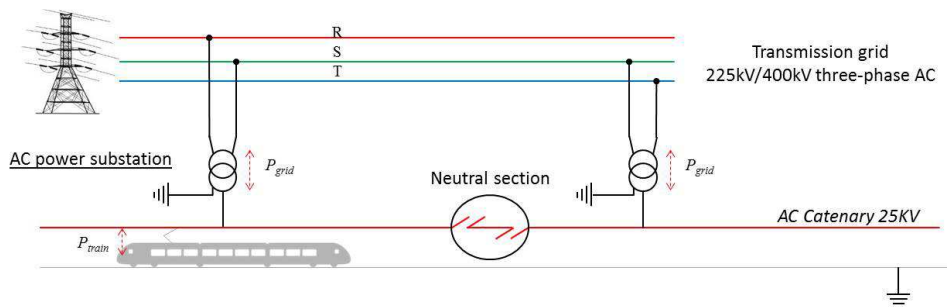


Fig. 1 Simple scheme of single-phase railway power supply system

A typical AC type HRPS is shown in Fig. 2, which includes the connection with transmission grid and also hybrid part. The hybrid part groups renewable energy resources and energy storage systems together through a DC bus, and then connected with the single-phase catenary via DC-AC converter and power transformer. The power can flow from catenary to DC bus and vice versa. The wind turbines are connected to DC bus via power converters, and they are controlled to extract maximum power. The charging/discharging of batteries depends on the electricity price as well as the local power balance situation.

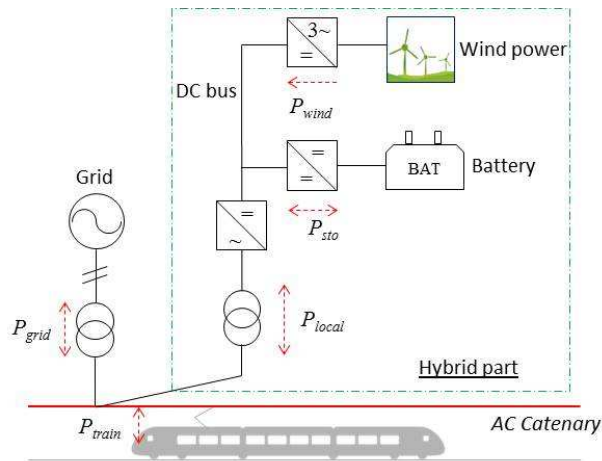


Fig. 2 Simple scheme of a hybrid railway power substation

3. Modelling and control of hybrid railway power substation

3.1. Sizing

The power substation Sarry located on the national high-speed line LN1 Paris-Lyon is selected to conduct the hybridisation. This AC type substation already reaches the maximum power limit at the connection point with the transmission grid. Besides, there is still pressure to increase train frequency on this line.

The optimal sizing of a HRPS can be solved by using CONIFER¹ based on the historical consumption profile and wind power prediction, which is a tool developed by another project of SNCF to select optimal subscribed power of RPS and size HRPS, to minimise the operation cost. A typical daily consumption profile is shown in Fig. 3. The optimal sizing results for a horizon of 20 years are listed in Table 1.

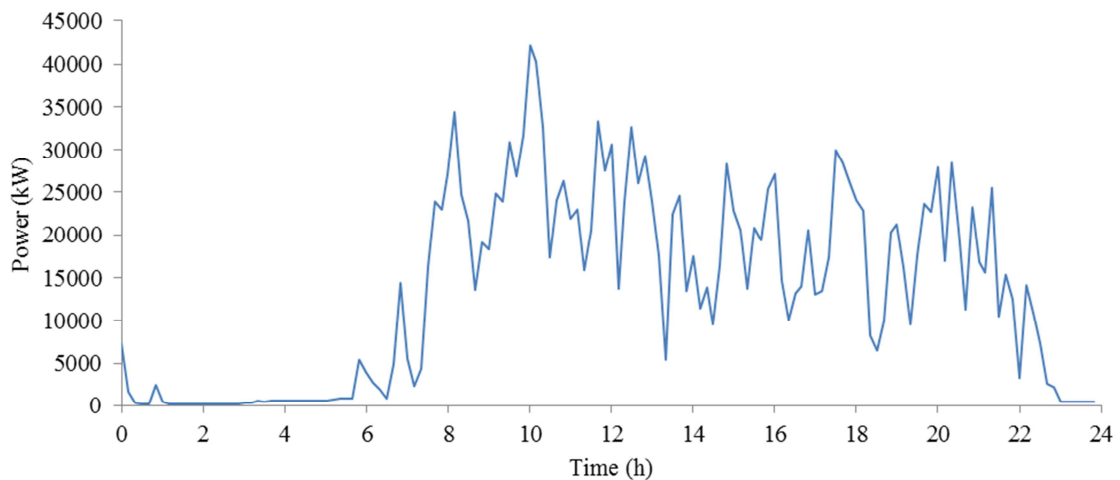


Fig. 3 Daily load profile of the power substation Sarry

¹ <http://www.conifer.fr/>

Table 1. Sizing results of a HRPS

| Component | Unit | Power (kW) | Energy (kWh) |
|--------------|------|------------|--------------|
| Wind turbine | 11 | 1670 | - |
| Battery | 1 | 136.4 | 58 |

3.2. Modelling

This subpart describes the modelling of a HRPS, including the connection with transmission grid, the catenary, wind power system, and also battery energy storages.

3.2.1. Wind power system

The wind power system is composed of a wind turbine, a gearbox, an induction machine, as well as a three-phase rectifier. The mathematic model of a wind turbine with gearbox can be expressed as follows:

$$T_{\text{turbine}} = \frac{1}{2} C_T \rho S R V_{\text{wind}}^2 \quad (1)$$

$$J \frac{d}{dt} \Omega_{\text{turbine}} = T_{\text{turbine}} - T_{\text{shaft}} - f \Omega_{\text{turbine}} \quad (2)$$

$$\begin{cases} \Omega_{\text{gb}} = k_{\text{gb}} \Omega_{\text{shaft}} \\ T_{\text{shaft}} = k_{\text{gb}} T_{\text{gb}} \end{cases} \quad (3)$$

where S is the area swept by the blades; ρ is the air density; and R is radius of the blades. The torque coefficient C_T is a nonlinear function of tip-speed ratio, which depends on the aerodynamic feature of the wind turbine. J is the equivalent inertia of the shaft; T_{shaft} is the torque of the shaft connecting the wind turbine and gearbox; and f is the friction coefficient of the shaft. Ω_{gb} and T_{gb} are the angular speed and torque of the gearbox, respectively.

The average model of the electric machine and rectifier using RMS quantities is given as:

$$\begin{cases} L_s \frac{di_{\text{arm}}}{dt} = V_{\text{arm}} - R_s i_{\text{arm}} - e_{\text{arm}} \\ T_{\text{gb}} = k_m i_{\text{arm}} \end{cases} \quad (4)$$

$$\begin{cases} V_{\text{dc}} = m_{\text{wind}} V_{\text{arm}} \\ i_{\text{arm}} = m_{\text{wind}} i_{\text{wind}} \end{cases} \quad (5)$$

where i_{arm} and V_{arm} are RMS values of the three-phase armature current and voltage, respectively; L_s and R_s are the armature inductance and resistance; e_{arm} is the back electromotive force (EMF), and k_m is the torque coefficient. m_{wind} is the equivalent modulation ratio; V_{dc} is the DC bus voltage; and i_{wind} is the output current of the wind power system.

3.2.2. Battery storage system

The battery system is connected to the DC bus via a step-up chopper to allow the charging and discharging. Its output voltage can be calculated by the no-load voltage and the inner resistance, which is a nonlinear function of the State of Charge (SoC). The model of battery system with DC-DC converter is given as:

$$L_{\text{bat}} \frac{di_{\text{bat}}}{dt} = V_{\text{bat}} - V_{\text{chop}} - R_{\text{bat}} i_{\text{bat}} \quad (6)$$

$$\begin{cases} V_{\text{chop}} = m_{\text{bat}} V_{\text{dc}} \\ i_{\text{bat}} = m_{\text{bat}} i_{\text{sto}} \end{cases} \quad (7)$$

where V_{chop} and V_{bat} are the high-voltage and low-voltage sides of the DC-DC converter, respectively; i_{bat} is the

current flowing out the battery; L_{bat} and R_{bat} are the inductance and corresponding resistance of the inductor. m_{bat} is the modulation ratio of DC chopper, which is limited between 0 and 1; and i_{sto} is the output current of the energy storage system.

3.2.3. AC catenary and the grid converter

The single-phase AC catenary is powered by high-voltage transmission grid via a power transformer, and also the DC bus via power converters. The electric grid is assumed to be infinite, thus the catenary voltage is constant and guaranteed by electric grid. The current balance at the AC catenary is given as:

$$i_{train} = i_{grid} + i_{cat} \quad (8)$$

where i_{train} represents the current consumed by the train; and i_{cat} represents the current flowing into the catenary from DC bus.

The dynamics of the DC bus is modelled as:

$$i_{local} = i_{wind} + i_{sto} \quad (9)$$

$$C_{dc} \frac{dV_{dc}}{dt} = i_{local} - i_{dc} \quad (10)$$

where i_{local} is the total current supplied by the local energy sources; and i_{dc} is the DC side current of the DC-AC converter. The power converter at the coupling of AC and DC is modelled as:

$$\begin{cases} V_{conv} = m_{bus} V_{dc} \\ i_{dc} = m_{bus} i_{cat} \end{cases} \quad (11)$$

$$L_{conv} \frac{di_{cat}}{dt} = V_{conv} - V_{cat} \quad (12)$$

where m_{bus} is the average modulation ratio of the converter; L_{conv} represents inductance of the power converter; V_{conv} is the RMS value of single-phase AC voltage.

3.3. Representation and control

The model of multi-source system can be properly represented by Energetic Macroscopic Representation (EMR) proposed by (Bouscayrol, et al., 2000). It respects the causality principle and uses some basic blocks, such as source, conversion element with/without energy accumulation to represent the whole system. One of the advantages is that EMR provides us a general representation method for complex systems with multiple sources. Another point is that the corresponding control structure called Inversion Based Control (IBC) can be directly deduced from EMR of the system, which gives us the opportunity to design controllers systemically. The EMR of the studied HRPS is shown in Fig. 4.

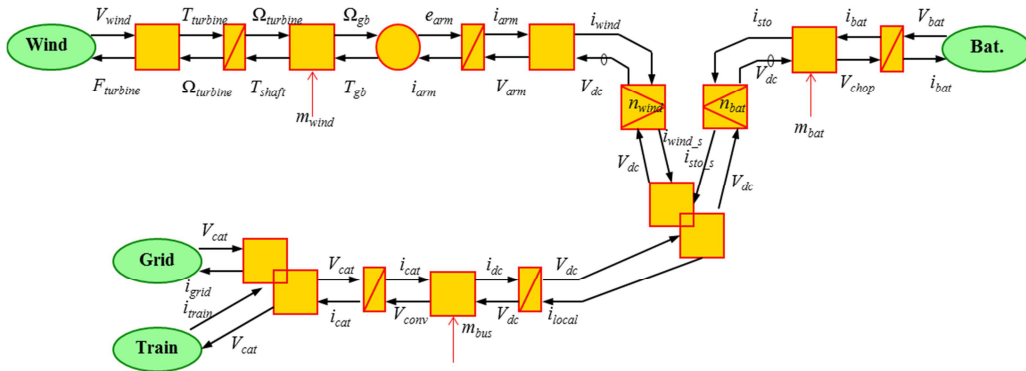


Fig. 4 EMR of the studied HRPS

Applying inversion principle, the corresponding IBC of the studied HRPS is shown in Fig. 5. MPPT algorithm is

adopted to maximize the production of wind power system. The battery is controlled in current mode, and the current reference is calculated by EMS, while the DC bus voltage is regulated by DC-AC converter.

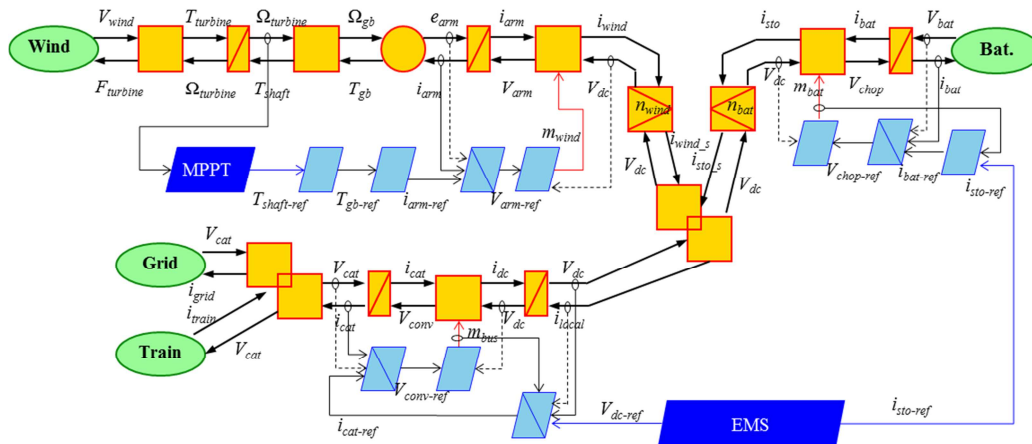


Fig. 5 IBC of the studied HRPS

3.4. Energy management system

EMS is constructed to realise optimal energetic management, in order to reduce the electricity bill, as well as guarantee the life-time span of batteries. It takes consideration the power balance at HRPS, the electricity price, the production of wind power as well as SoC of batteries, to calculate optimal charging/discharging power of batteries. For example a hierarchical structure combining linear/nonlinear programming and fuzzy logic controller can be adopted to generate battery current reference, proposed by (Pankovits, Pouget, Robyns, Delhaye, & Brisset, 2014).

3.5. Simulation results

The system model is constructed in Matlab/Simulink to conduct numerical simulations. One typical daily power consumption profile of the studied substation, the corresponding wind speed, and also electricity price in 2013 are selected. The simulation results are shown in Fig. 6. The DC bus voltage is controlled to be constant 1.5 kV and the battery charges and discharges according to the electricity price. The SoC of the battery is controlled between 0.3 and 0.9 to avoid deep discharge, such that a longer life-span can be obtained.

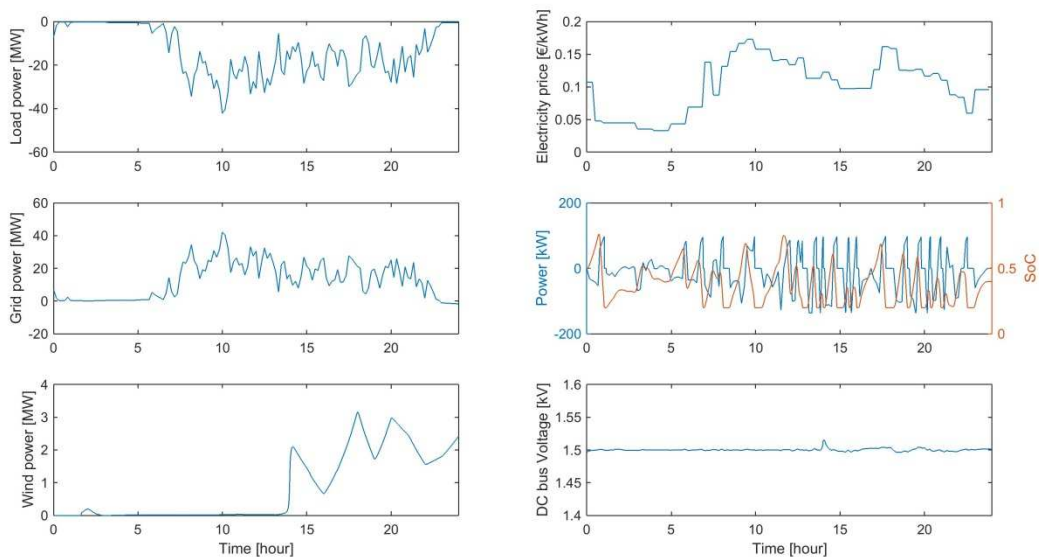


Fig. 6 Simulation results of the studied HRPS

4. Hardware-in-the-loop test

4.1. Configuration

To reduce the development cost and time, a reduced-scale power HIL platform is constructed in our laboratory to test the proposed concept. As shown in Fig. 7, the battery system and the corresponding power converter are replaced by an ENERSYS Lead acid battery and an IGBT based DC-DC converter. The other parts are simulated in a real-time simulator. The simulation part is connected to the real part via a power interface, which is a bidirectional power source controlled by the simulator. It connects electrically simulation part and real part, as well as takes the scale into consideration in reduced-scale HIL test.

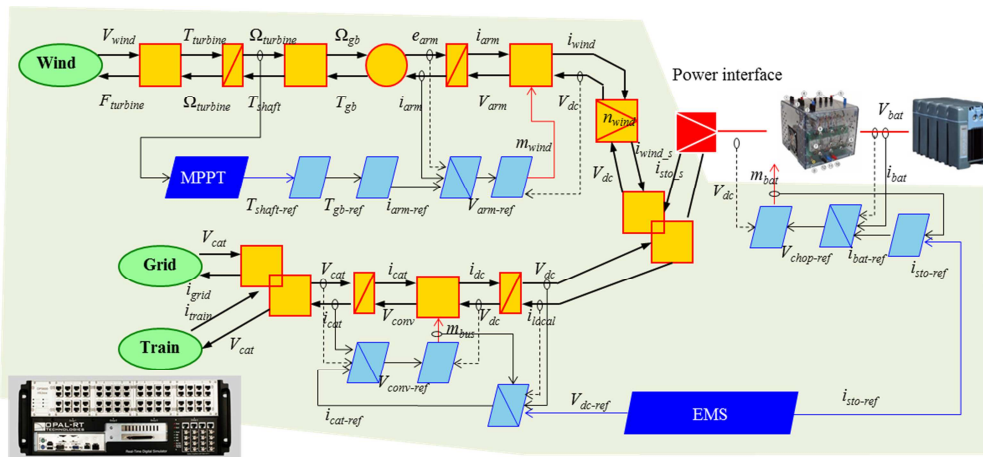


Fig. 7 Reduced-scale power HIL structure

The lead acid battery has a typical output voltage 48 V, a typical energy 3.9 kWh at 25°C, with the maximum continuous discharging current 44 A and charging current 32 A. The power interface is implemented by a controllable bipolar power supply KIKUSUI PBZ40-10, which can work in constant-voltage (CV) mode and constant-current (CC) mode. In this test, the power supply is controlled externally in CV mode by the real-time simulator via analogic signal (-10 V to 10 V).

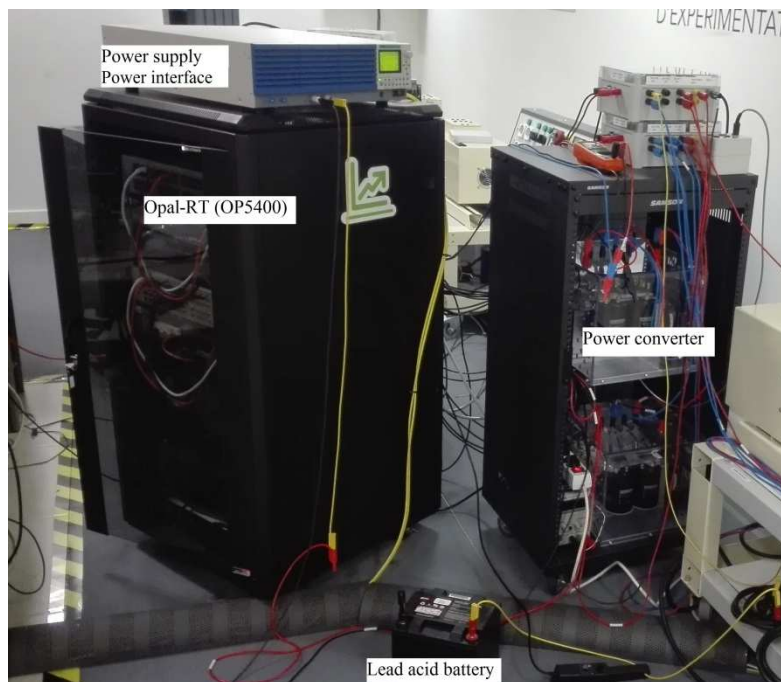


Fig. 8 Photograph of the platform in SNCF I&R energy laboratory

A photograph of the platform in SNCF I&R energy laboratory is shown in Fig. 8. The power supply has voltage limits between ± 40 V, as well as current limits ± 10 A, thus only a reduced-scale power HIL can be carried out. The voltage scale is selected 1500:40 to limit DC bus voltage to 40 V, while the scale for current is 90:5 to limit discharging/charging current in 5 A, thus the power scale is 675:1. An Opal-RT real-time simulator OP5400 is used to carry the numerical simulation part in real-time, which control the voltage of power supply through analogic signal. The battery is controlled in current mode, which follows the reference coming from EMS.

4.2. Experimental results

One HIL test with battery is conducted with the same profiles as used in numerical simulation. Since only a real battery is adopted, and others are simulated in Opal-RT, the power produced by wind turbines, supplied by transmission grid and the consumption curves would be identical as those of numerical simulation. The power profiles of batteries in simulation and HIL test are compared in Fig. 9. The experimental results are rescaled to be comparable to simulation results.

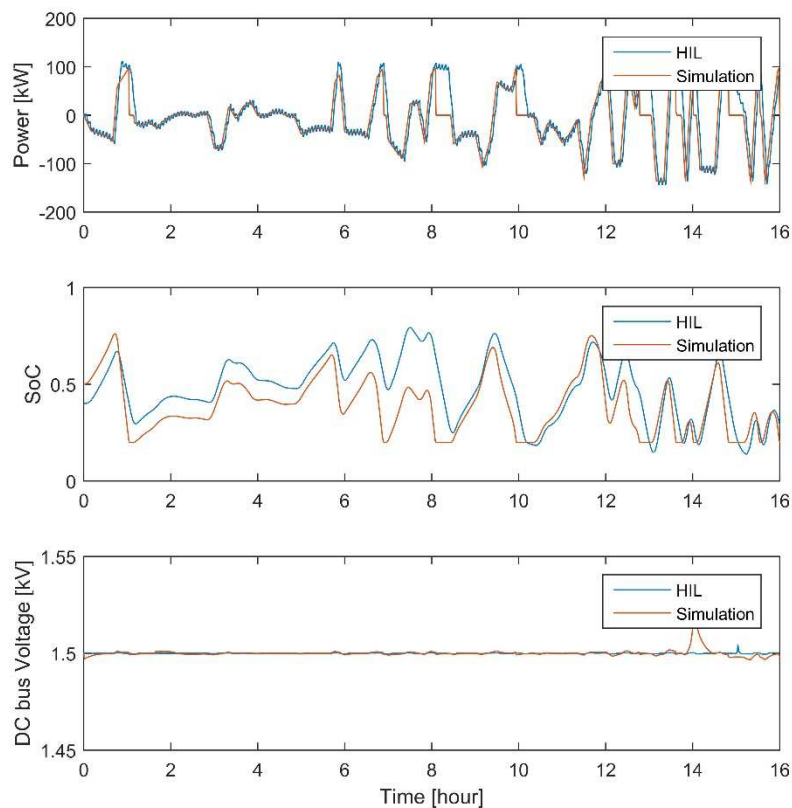


Fig. 9 Comparison of HIL test and simulation results

It can be seen that HIL test results are close to those of simulation, which confirms the effectiveness of our simulation model and the corresponding EMS. When the power is positive, the battery discharges while it charges when the power is negative. The differences between simulation and HIL test results are due to the initial SoC of battery, as well as current measurement. The SoC of battery is controlled between 30% and 90%, thus discharging power is enforced to zero when SoC is too low at around 8h in simulation; while the SoC of battery is still over 30% in HIL test, which allows the battery continues to discharge.

Conclusion

This paper has developed the real-time simulation model of HRPS, in order to study the energy management system and also the dynamics of battery system. A power HIL platform has been constructed to test the proposed

model and experimental results have verified its effectiveness. EMR is useful to organise the complex system, to deduce a systemic control structure, and also HIL test. In the future, the dynamics of power electronics, power transformers as well as the interaction between catenary and the trains will be considered, such that a more precise HRPS emulator would be available for the test of HRPS controller.

Appendix

The basic elements of EMR and IBC are given in Table 2.

Table 2 Basic elements of EMR and IBC

| Source | Converter with energy accumulation | Mono-domain converter | Multi-domain converter | Mono-domain coupling | Multi-domain coupling |
|--------|-------------------------------------------------|------------------------|------------------------|-----------------------|-----------------------|
| | | | | | |
| | Inversion of converter with energy accumulation | Inversion of converter | | Inversion of coupling | |
| | | | | | |

References

- Bouscayrol, A., Davat, B., Fornel, B. d., François, B., Hautier, J. P., Meibody-Tabar, F., et al. (2000, May). Multimachine Multiconverter System: application for electromechanical drives. *European Physics Journal - Applied Physics*, 10(2), 131-147.
- Commissariat général au développement durable. (2016). *Chiffres clés du transport - Edition 2016*. La Défense: Ministère de l'Environnement, de l'Energie et de la Mer.
- Nasr, S., Iordache, M., & Petit, M. (2015). Smart micro-grid integration in DC railway systems. *Proc. of IEEE PES Innovative Smart Grid Technologies Conference Europe*, (pp. 1-6).
- Ogura, K., Nishimura, K., Matsumura, T., Tonda, C., Yoshiyama, E., Andriani, M., et al. (2011). Test results of a high capacity wayside energy storage system using Ni-MH batteries for DC electric railway at New York City Transit. *Proc. of IEEE Green Technologies Conference*, (pp. 6-11).
- Pankovits, P., Ployard, M., Pouget, J., Brisset, S., Abbas, D., Robyns, B., et al. (2013). Design and Operation Optimization of a Hybrid Railway Power Substation. *Proc. of European Conference on Power Electronics and Application*, (pp. 1-8).
- Pankovits, P., Pouget, J., Robyns, B., Delhaye, F., & Brisset, S. (2014). Towards railway-smartgrid: Energy management optimization for hybrid railway power substations. *Proc. IEEE PES Innovative Smart Grid Technologies Conference Europe*, (pp. 1-6).
- Radcliffe, P., Wallace, J., & Shu, L. (2010). Stationary applications of energy storage technologies for transit systems. *Proc. of IEEE Electrical Power and Energy Conference*, (pp. 1-7).
- SNCF. (n.d.). *L'engagement de SNCF entre 2014 et 2025*. Retrieved 9 12, 2017, from <http://www.sncf.com/fr/rse/bilan-carbone>